Culling avalanches in bootstrap percolation

C. Farrow and P. M. Duxbury
Physics and Astronomy Department, Michigan State University, East Lansing, Michigan 48824, USA

Cristian F. Moukarzel
Departamento de Física Aplicada, CINVESTAV del IPN, 97310 Mérida, Yucatán, Mexico
(Received 2 August 2005; published 8 December 2005; publisher error corrected 12 December 2005)

We study the culling avalanches which occur after the "death" of a single randomly chosen site in a network where sites are unstable, and are culled, if they have coordination less than an integer parameter m. Avalanche distributions are presented for triangular and cubic lattices for values of m where the associated bootstrap transitions are either first or second order. In second order cases, the culling avalanche distribution is found to be exponential, while in first order cases it follows a power law. We present an exact relation between culling avalanches and conventional bootstrap percolation and show that a relation proposed by Manna [Physica A **261**, 351 (1998)] can be a good approximation for strongly first order bootstrap transitions but not for continuous bootstrap transitions.

DOI: 10.1103/PhysRevE.72.066109 PACS number(s): 02.50.−r, 07.05.Kf, 05.50.+q, 64.60.Ak

I. INTRODUCTION

Bootstrap percolation (BP) [1,2] is a modified form of a scalar percolation in which a lattice is randomly populated with a fraction p of present sites; and all sites without a suitable number of present neighbors are then iteratively removed, or culled. The original motivation for the BP model came from a consideration of magnetic materials where atoms require a minimum connectivity in order to maintain their magnetic alignment. BP is studied under another name in graph theory where the infinite cluster in BP corresponds to the giant m core [3], and has applications to complex networks and dense storage arrays [4].

The smallest possible, elementary, culling avalanches occur when a single randomly chosen site dies or is "burnt." By alternating between burning sites and culling, we analyze the evolution of elementary bootstrap avalanches beginning with a complete lattice and ending when the lattice is empty. The process of random death and culling has a variety of physical interpretations, including radiation damage of random networks of interest in material science, species extinctions in biological networks, and random outages or failures in communication or transportation networks. There are also relations to avalanches in magnetic systems which lead to observable noise, for example, Barkhausen noise in the case of hysteresis loops. In fact bootstrap percolation is related to the weak disorder limit of one of the key models of disordered magnets, the random field Ising model (RFIM) [5]. Another motivation for studying culling avalanches is to use these avalanches to rapidly locate and analyze bootstrap percolation critical behavior. This possibility has been raised by Manna and co-workers [6]. We find that in general it is difficult to identify the bootstrap threshold using avalanches alone, though if the transition is strongly first order the avalanche method is effective.

Numerical approaches to bootstrap percolation have to be subjected to strong scrutiny as metastability effects lead to very strong finite size scaling corrections to the asymptotic behavior in some cases. For $m>z/2$, where z is the lattice coordination number, the bootstrap percolation threshold is asymptotically at $p_c=1$ and the percolative transition is strongly first order. Moreover, for $m=z/2+1$, interesting rigorous mathematical treatments have shown that there are logarithmic size effects which lead to values of p_c that can be significantly smaller than 1 even for large lattices [7–10]. Special numerical methods are required to probe these finite size effects [11,12]. The cases $m\leqslant z/2$ for square, triangular, and cubic lattices have $p_c<1$ and a continuous bootstrap transition. These cases are well behaved numerically and are consistent with conventional percolation, though with shifted values of the percolation threshold. However, the case $z=m/2$ exhibits its asymptotic critical behavior only at very large lattice sizes so that early numerical work on smaller lattices, which suggested nonuniversal exponents that depend on m, is now believed to be unreliable [13–17]. The most recent, extremely large, simulations support the idea that all of the continuous bootstrap transitions on these lattices are universal and in the same universality class as conventional percolation. The most interesting cases are then $m=z/2$ and $m=z/2+1$ and we present a detailed analysis of elementary avalanches for these two cases on triangular and cubic lattices.

This paper is organized as follows. In Sec. II we give a careful discussion of the avalanching bootstrap percolation (ABP) algorithm, and demonstrate that the avalanche procedure has an exact correspondence with conventional bootstrap percolation. Section III contains the analysis of elementary bootstrap avalanches on triangular and simple cubic lattices. Section IV contains a summary of our main results and a brief discussion.

II. ALGORITHMS FOR BOOTSTRAP AVALANCHES

For a given lattice an m-culling procedure (mCP) consists of recursively removing all sites which have fewer than m neighbors. At the completion of an mCP all sites have at least m neighbors. This set of sites is called the stable cluster

configuration (SCC) or m core. This is exactly the same as the m core in the core percolation problem studied in graph theory [5]. The sites that have been removed during a bootstrap avalanche are called the culled sites. An mCP is Abelian [6] in that any culling order can be used as long as only sites with fewer than m neighbors are culled and at completion there are no sites with fewer than m neighbors.

A spanning cluster is a cluster in the m core which spans the sample under consideration. At the onset of bootstrap percolation a spanning cluster emerges in the SCC. On random graphs, a spanning cluster is not well defined. Instead the emergence of a giant m-core cluster is considered [3]. A giant cluster is a stable cluster that contains a finite fraction of the sites of the original lattice. In conventional bootstrap percolation, the initial configuration consists of a lattice where each site is present independently of all other sites with probability p. The mCP is applied to this configuration. The m-bootstrap percolation threshold is the largest value of p at which the m core that remains after culling does not contain a spanning cluster (or a giant cluster). Connectivity percolation [18] is the $m=1$ limit of this procedure. First we define a procedure which is equivalent to conventional bootstrap percolation, but which enables a more straightforward generalization to ABP and also to an understanding of the correction required to make Manna's method [6] precise.

The following procedure is equivalent to conventional bootstrap percolation.

Procedure 1 (BP procedure for finding p_c). For a given lattice with N sites, randomly assign a unique integer label, $l_i=1,\ldots,N$, to each site. This initial labeling, or ordering, of the sites is referred to as the initial configuration (IC). Set the index $k\leftarrow 0$. Then,

(1) $k\leftarrow k+1$.

(2) Burn (remove) all sites with labels $l_i\leqslant k$.

(3) Apply the mCP and check the resulting SCC for a spanning cluster.

(4) If a spanning cluster does not exist EXIT. If a spanning cluster exists, restore the lattice to the IC and go to 1.

The final value of k found in this way, k_c, gives the m-BP threshold,

$$p_c = 1 - \frac{k_c}{N}. \tag{1}$$

Now we present an avalanche algorithm, ABP1, which also finds p_c exactly. This procedure was originally introduced by Manna [6], though the way he calculated p_c from it contains a misconception which is easily corrected as shown below. The procedure is similar to the BP procedure above, except that the lattice is not restored to the IC after each trial.

Procedure 2 (ABP1 procedure for finding p_c). Start with the same IC as for the BP procedure and define a time variable, $t\leftarrow 0$.

(1) Burn (remove) the site on the SCC with the lowest label, k'. $t\leftarrow t+1$.

(2) Apply the m-culling procedure and check the resulting SCC for a spanning cluster.

(3) If a spanning cluster exists, go to 1. If a spanning cluster does not exist EXIT.

The values of k' and t when the algorithm exits are referred to as k_c' and t_c, respectively.

In the ABP1 procedure the index t counts the number of sites which die (i.e., are removed) before percolation ceases. Our definition of t_c is equivalent to Nf_c^* as defined by Manna [6], who goes on to argue that $p_c=1-f_c^*$, which we prove to be generally false below. Data are presented in Sec. III to further demonstrate this fact. For a given IC the m core after the removal of the site labeled n in the ABP1 procedure is the same as that produced after the nth loop of the BP procedure. This implies $p_c\leqslant 1-t_c/N$.

The equivalence of BP and ABP1 is evident from the Abelian nature of bootstrap percolation [6]. That is, bootstrap percolation involves two processes, the first is random site removal (which is equivalent to death or burning) and the second is culling. There are then two ways in which bootstrap percolation is Abelian. First, it does not matter the order in which unstable sites are culled. Second, it does not matter the order in which sites are removed. The final state is only determined by the list of n sites removed and the culling, in arbitrary order, of all unstable sites. In other words, the SCC does not depend on the path taken to reach the final stable state. There is, however, a subtle difference between BP and ABP1, which arises due to the fact that ABP1 includes the possibility of removing a site, which we label a redundant site, that has already been culled at an earlier stage of the algorithm. Exact counting of these redundant sites, $R(t)$, is key to a correct correspondence between conventional bootstrap percolation and bootstrap avalanches. Before calculating the number of redundant sites, we introduce a third algorithm that is more efficient than ABP1.

The ABP1 procedure as presented above is inefficient because a breadth first search is required to test for percolation after each step in the procedure. Generally a half-interval search technique is employed to find p_c using the BP procedure [19] and a similar technique can be used with the ABP1 procedure. In the ABP1 case, the lattice is completely evacuated using the ABP1 procedure without checking for percolation and each site in an avalanche is given the label of the avalanche seed site. These avalanche clusters are then added or removed from the lattice using a half-interval search to locate k_c.

In terms of storage, giving every site a random label, as required by the ABP1 procedure, is also memory inefficient. To avoid using an integer label on each site, we instead define each site to be either *present, culled*, or *burned*. Burned sites are those which seed a culling avalanche. Present sites contribute to the SCC. A site that is not present is referred to as absent. A site can be made absent by being culled or by being burned.

Using these definitions, we define a more efficient implementation of the avalanche algorithm, which we call ABP2. We assign to each site two binary variables, $b_i=0,1$ and $c_i=0,1$. If $b_i=1$, a site has been burned and if $c_i=1$, a site has been culled. A site is present if $b_i=0$ and $c_i=0$.

Procedure 3 (ABP2 for finding p_c). For a given lattice with N sites, start with $b_i=0$ and $c_i=0$ for every site and set $t=0$ and $R(0)=0$.

(1) From the set of sites with $b_i=0$ randomly choose one, label it j, and set its value to $b_j=1$. That is, burn that site. If

that site has already been culled (i.e., $c_j=1$) set $R(t)=R(t)+1$ and return to 1. If site j has not been culled, $t \leftarrow t+1$, set $R(t)=R(t-1)$ and proceed to 2.

(2) Apply mCP and for any site that is culled in this avalanche set $c_i=1$. The number of sites which are culled in this avalanche is $a(t)$.

(3) If a spanning cluster exists, go to 1. If a spanning cluster does not exist EXIT.

The function $R(t)$, the number of redundant burns, is the number of times that the procedure tries to burn a site that is already culled at a time up to and including time t, and plays an important role in determining the relation between ABP and BP. In particular, the redundant sites are sites that would have been removed in the random dilution process that precedes the usual mCP in BP. The total number of burned sites is then $B(t)=t+R(t)$, so that

$$1-p=\frac{B(t)}{N}=\frac{1}{N}[t+R(t)]=\frac{k}{N}, \tag{2}$$

which gives the relation between BP, ABP1, and ABP2. The total number of culled sites is given by

$$C(t)=\int_0^t a(t)dt, \tag{3}$$

and the number of redundant burns at time t is

$$r(t)=\frac{dR(t)}{dt}. \tag{4}$$

The ABP2 procedure requires at least two bits of storage for each site. This is twice as much as BP done with the multispin coding technique [20,21], but it is comparable in terms of speed. It will be shown below that for continuous BP systems the avalanche size stays relatively small throughout the ABP procedure. Since only the neighborhood of the avalanche is checked against the culling condition the average time spent in generating a culling avalanche is typically $O(1)$. Thus, using a half-interval search technique it takes $O(N)$ time to evacuate the lattice and an additional $O(N\ln(N))$ time to find p_c for a given IC. The total time is $O(N\ln(N))$, which includes the time $[O(N)]$ it takes to label the clusters of the SCC [22].

It would be useful if the ABP procedure could identify the bootstrap percolation point without the use of a half-interval search, and this was the reason that Manna originally introduced the procedure [6]. Such an analysis would not require the costly identification of percolation clusters and would require $O(N)$ time to record the relevant avalanche information of the system. We show in Sec. III that in the case of first order transitions it is possible to identify p_c quite accurately from the ABP avalanches; however, it is more difficult for second order bootstrap cases.

The procedures as defined above terminate once the lattice no longer percolates. However, we are also interested in the avalanches after percolation and in the data presented in Sec. III we continue the ABP procedure until the lattices are completely empty.

III. NUMERICAL RESULTS

Results for elementary avalanches in bootstrap percolation for triangular and cubic lattices are presented in Figs. 1–4. The data are generated by starting with undiluted triangular or simple cubic lattices and then applying the bootstrap avalanche algorithm ABP2 until the lattice is empty. Results are presented for the most interesting cases, $m=3$ and $m=4$.

The $m=3$ cases (Figs. 1 and 3), which exhibit a second order bootstrap percolation transition, display qualitatively different behavior than the $m=4$ cases which have a sharp first order bootstrap percolation transition (Figs. 2 and 4). In ABP the parameter t represents the number of "essential" burned sites, i.e., the total number of burned sites minus the redundant burned sites [i.e., $t=k-R(t)$]. We will often refer to t or $\tau=t/N$ as the time parameter and $\kappa=k/N$ is related to the conventional bootstrap percolation concentration p through $p=1-\kappa$.

Figures 1(a), 2(a), 3(a), and 4(a) show the deviation between the time parameter τ and κ. The difference $\kappa-\tau=R(t)/N$ is the number density of redundant burn operations. In these figures the vertical and horizontal dashed lines indicate the percolation threshold. For the triangular lattice with $m=3$ [Fig. 1(a)] $p_c=0.6291(5)$ [14] and is consistent with the value $\kappa_c=1-p_c=0.372(2)$ found from our simulations. The value of $\tau_c=0.338(2)$ we find indicates that at threshold the number of redundant sites removed $R(t)/N=\kappa_c-\tau_c=0.034(4)$. This is the error incurred in using τ_c instead of κ_c to find the bootstrap threshold using the ABP algorithm. The total number of burn operations, followed by culling, required to empty the lattice is $\tau_f=t_f/N=0.3832(2)$. This final time is quite precise for second order bootstrap problems. For the $m=3$ cubic lattice case, which is also second order [see Fig. 3(a)] we find $\kappa_c=0.427(2)$, $\tau_c=0.369(1)$, and $\tau_f=0.381(1)$. The percolation threshold value of $p_c=1-\kappa_c=0.573(2)$ is consistent with estimates found using conventional procedures [2,3,11,16]. The first order cases clearly show a different behavior than the second order cases. Instead of an upturn in κ vs τ [Figs. 2(a) and 4(a)], there is a downturn. This is due to the fact that there is considerable variability in τ_f for the first order cases. For each configuration there is a large avalanche that evacuates the lattice, and for a single configuration $\kappa=\tau$ to a good approximation up to $\tau_f=\tau_c$. These cases are known to have very strong size effects, so that although the value of $\kappa_c=1-p_c$ is found to be finite in Figs. 2(a) and 4(a), it is expected that $\kappa_c \to 0$ logarithmically in the large lattice limit [7–10].

The cummulative culling avalanche distributions are presented in Figs. 1(b), 2(b), 3(b), and 4(b). In the first order cases [Figs. 2(b) and 4(b)] the avalanche distribution is broad and has a power law tail, while in the second order cases [Figs. 1(b) and 3(b)] the avalanche distribution has an exponential tail and most avalanches have finite size. We have searched for an indication of the onset of percolation in the tails of these distributions and have found no clear indicator of new behavior near p_c. For example, it is evident from Fig. 3(b) that even at p_c the culling avalanche distribution is not a power law in this second order case. In second order cases,

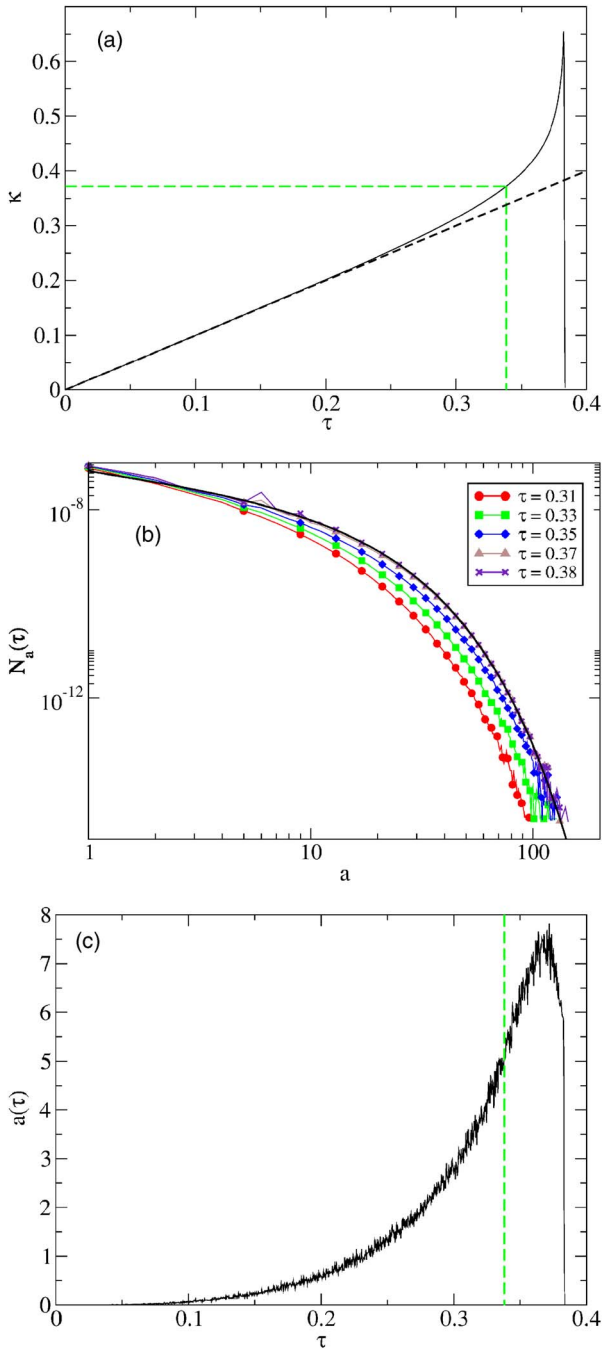

FIG. 1. (Color online) Bootstrap avalanche behavior for $m=3$ on a triangular lattice of size $L=1024$ with periodic boundary conditions. (a) The number of burned sites $B(t)/N=\kappa$ (solid line) as a function of the normalized time parameter $\tau=t/N$. The angled dashed line corresponds to $\kappa=\tau$, so that the difference between this dashed line and the solid line is the number of redundant burned sites $R(\tau)/N$—see Eq. (2). (b) The cumulative avalanche distribution $N_a(\tau)$ for a range of values of τ as indicated in the legend. The data are well described by Eq. (5). The solid line is a fit of the $\tau-0.38$ data using Eq. (5) with $c_1(\tau)=9.0\times10^{-08}$, $x(\tau)=0.88$, and $c_2(\tau)=0.105$. (c) The average avalanche size as a function of τ. The vertical and horizontal dashed lines in (a) and (c) give the location of the critical point $\tau_c=0.338(2)$ and $\kappa_c=0.372(2)$.

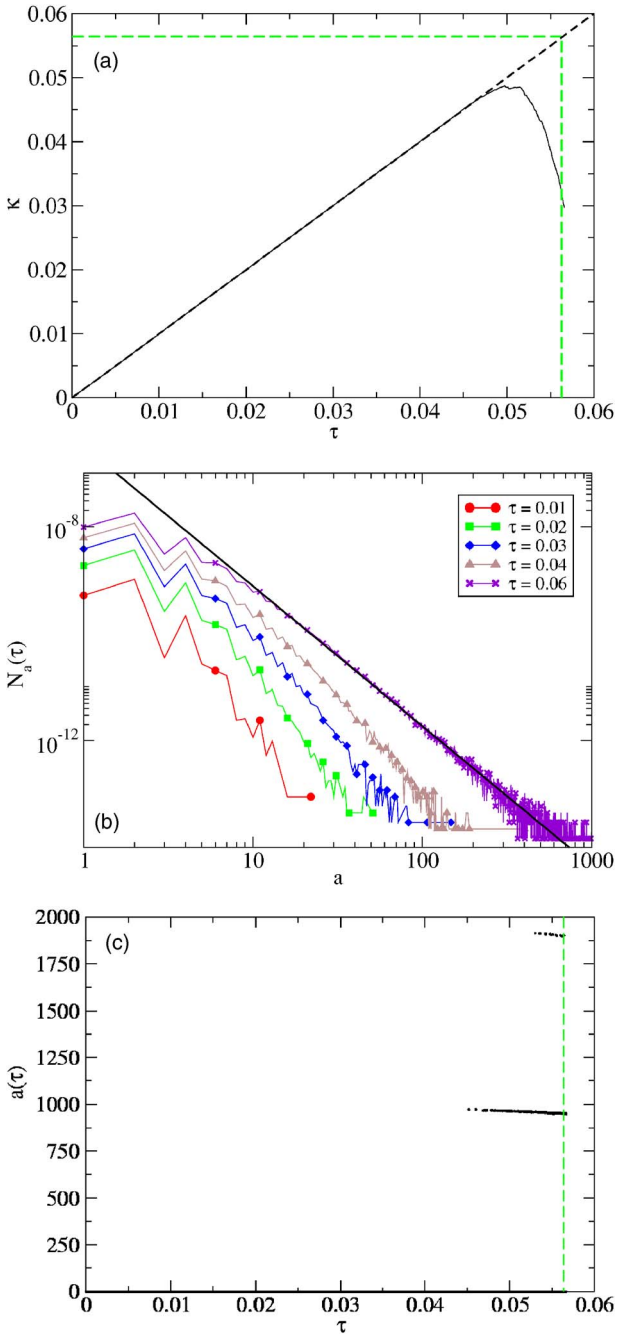

FIG. 2. (Color online) Bootstrap avalanche behavior for $m=4$ on a triangular lattice of size $L=1024$ with periodic boundary conditions. (a) The number of burned sites $B(t)/N=\kappa$ (solid line) as a function of the normalized time parameter $\tau=t/N$. The dashed line is the curve $\kappa=\tau$. The downturn for large τ is due to strong fluctuations in τ_f. The vertical and horizontal dashed lines give the location of the critical point at $\tau_c=0.056(3)=\kappa_c$. (b) The cumulative avalanche distribution $N_a(\tau)$ for a range of values of τ as indicated in the legend. The data are well described by Eq. (6). The solid line is a fit of the $\tau_f=0.06$ data using Eq. (6) with $c_3(\tau)=7.7\times10^{-07}$ and $y(\tau)=2.54(4)$. (c) The average avalanche size as a function of τ. The vertical dashed line gives the location of the critical point. The steplike nature of the distribution is due to the occurence of extensive avalanches which are not included in the power law distribution presented in (b).

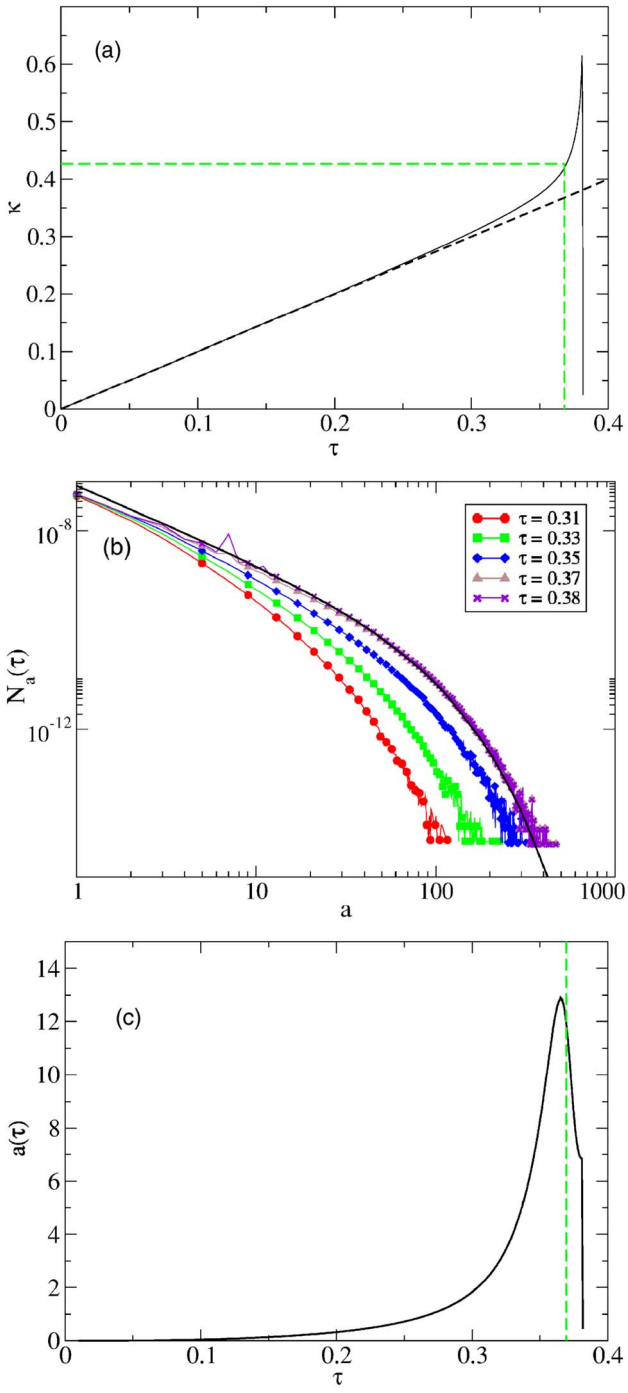

FIG. 3. (Color online) Bootstrap avalanche behavior for $m=3$ on a cubic lattice of size $L=128$ with periodic boundary conditions. (a) The number of burned sites $B(t)/N=\kappa$ (solid line) as a function of the normalized time parameter $\tau=t/N$. The dashed line is the curve $\kappa=\tau$ so that the difference between the dashed and solid lines is the number of redundant burned sites $R(\tau)/N$, see Eq. (2). (b) The cumulative avalanche distribution $N_a(\tau)$ for a series of values of τ as indicated in the legend. The data are well described by Eq. (5). The solid line is a fit of the $\tau=0.38$ data using Eq. (5) with $c_1(\tau)=7.2\times10^{-08}$, $x(\tau)=0.62(1)$, and $c_2(\tau)=0.107$. (c) The average avalanche size $a(\tau)$ as a function of τ. The vertical and horizontal dashed lines in (a) and (c) give the location of the critical point $\tau_c=0.369(1)$ and $\kappa_c=0.427(2)$.

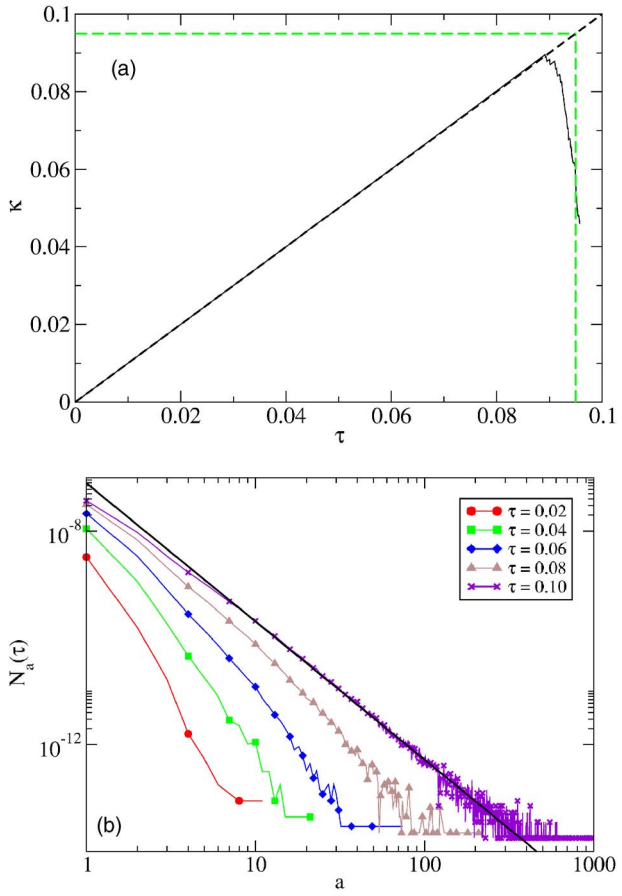

FIG. 4. (Color online) Bootstrap avalanche behavior for $m=4$ on a cubic lattice of size $L=128$ with periodic boundary conditions. (a) The number of burned sites $B(t)/N=\kappa$ (solid line) as a function of the normalized time parameter $\tau=t/N$. The dashed line is the curve $\kappa=\tau$. The downturn at large τ is due to strong fluctuations in τ_f. The vertical and horizontal dashed lines give the location of the critical point, $\tau_c=\kappa_c=0.096(1)$. (b) The cumulative avalanche distribution $N_a(\tau)$ for a series of values of τ as indicated in the legend. The data are well described by Eq. (6). The data are well described by a power law; for example, the solid line is a fit of the $\tau=0.10$ data using Eq. (6) with $c_3(\tau)=7.9\times10^{-08}$ and $y(\tau)=2.6(2)$.

we found that the cummulative distribution is well described by the function

$$N_a(\tau) = c_1(\tau)a^{-x(\tau)}\exp[-c_2(\tau)a] \tag{5}$$

and fits to this equation are presented in Figs. 1(b) and 3(b). In the first order cases [Figs. 2(b) and 4(b)], the tail of the cummulative culling distribution is a power law, with an exponent that varies with τ, so that

$$N_a(\tau) = c_3(\tau)a^{-y(\tau)} \tag{6}$$

where $y(\tau)$ is larger for small τ. However, we find that at the completion, the exponent $y(\tau_f)$ is close to the value 5/2 for the $m=4$ cases on both the triangular and cubic lattices.

Figures 1(c), 2(c), and 3(c) present the average avalanche size as a function of τ. In the first order cases [e.g., Fig. 2(c)], the average avalanche size is completely dominated by an extensive avalanche so that the average avalanche size is

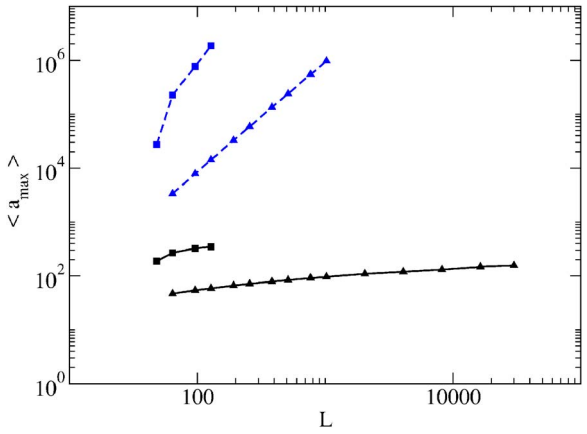

FIG. 5. (Color online) Finite size scaling behavior of the largest culling avalanche for (starting from the bottom of the figure) $m=3$ on a triangular lattice, $m=3$ on a cubic lattice, $m=4$ on a triangular lattice, and $m=4$ on a cubic lattice. The $m=3$ triangular case scales logarithmically with size, while the $m=4$ cases scale with L^d, where d is is the spatial dimension.

large once one sample in the set exhibits its extensive avalanche. In contrast, in the second order cases [Figs. 1(c) and 3(c)] the average avalanche size is a relatively smooth function of τ. We have found no indication of p_c in $a(\tau)$ from data such as this. In addition we looked at the fluctuations of $a(\tau)$, which is the avalanche susceptibility and also found no evidence of criticality.

A clear demonstration of the difference between first order and second order bootstrap culling avalanches is presented in Fig. 5, which shows the size of the largest avalanche as a function of the inverse of the system size L. In the second order cases ($m=3$ triangular and cubic lattices) the largest avalanche grows logarithmically with system size $\langle a_{max} \rangle \propto \ln L$, while in the first order cases ($m=4$ triangular and cubic lattices) the largest culling avalanche is proportional to the volume $\langle a_{max} \rangle \propto L^d$.

Another interesting feature of the cummulative distributions presented in Figs. 1(a)–3(b) is the presence of a nonmonotonic behavior at small avalanche sizes. This is due to small stable clusters and for the second order cases become more pronounced for $\tau > \tau_c$. In particular for the triangular lattice with $m=3$ [Fig. 1(b)] there is a peak at $a=6$, which is due to removing a site from a hexagonal cluster. The hexagonal cluster is the smallest stable finite cluster for $m=3$ triangular lattices. This is the most prevalent cluster in the SCC as the system approaches τ_f. Burning any site in this cluster leads to the culling of the whole cluster and a culling avalanche of size 6. The peaks at $a=9$, 11, 13, and 15 are similarly associated with stable clusters of size 10, 12, 14, and 16. Figure 6 shows the (small) clusters of size 7 and 10 that lead to avalanches of sizes 6 and 9, respectively. The 10-cluster gives an avalanche of size 9 if a gray site is removed. Any other removed site leads to an avalanche of size 2 and leaves a stable 7-cluster behind. Similarly for the cubic lattice the smallest stable cluster for $m=3$ is a cube of eight sites. This cluster leads to a peak in the avalanche distribution at an avalanche size of 7. As remarked above the onset of an extensive avalanche heralds the percolation threshold

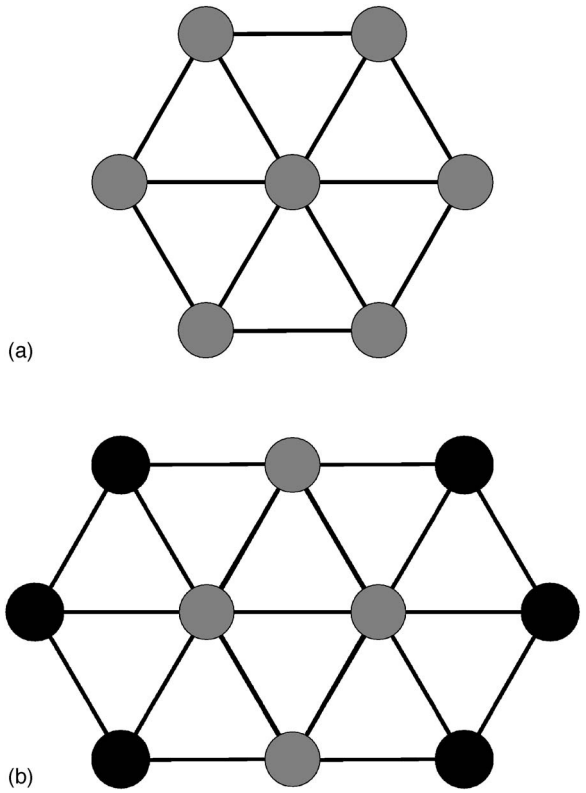

FIG. 6. The stable 7 and 10 clusters for $m=3$ on a triangular lattice. When a site on the 7 cluster is burnt a culling avalanche of size 6 results. When a black site on the 10 cluster is burnt a culling avalanche of size 2 occurs, while if a gray site on the 10 cluster is burnt an avalanche of size 9 results.

in first order bootstrap percolation problems. This enables identification of the bootstrap threshold from the ABP algorithm, as suggested by Manna [6]. However, we found that the largest culling avalanche does not necessarily occur near the bootstrap threshold in second order bootstrap problems. Similarly the peak in the average size of the culling avalanches does not occur at τ_c [see Figs. 1(c) and 3(c)]. However, the nonmonotonic behavior of the avalanche distribution which occurs even in second order cases is indicative of the correlated nature of bootstrap percolation culling process. We tested whether the peaks in the cummulative distribution have a behavior which changes its nature at the bootstrap percolation threshold. Figure 7 shows three probability curves for $m=3$ on a triangular lattice. The solid curve shows the probability of having an avalanche of size 6, $P_6(\tau)$. The dotted curve shows the probability that an avalanche of size 6 occurs on the largest cluster. The initial rise of the curve represents the increasing likelihood of having a nonzero avalanche as the SCC becomes less stable to burning and culling. The sharp decline is due to the imminent fractal structure of the SCC. Larger avalanches are becoming much more likely around the maximum of this curve. We can define the percolation threshold as the point of inflection in this curve right after the maximum. This is analogous to the definition of p_c through the probability of finding a site on the largest cluster in scalar percolation.

The dashed curve shows the probability of having an avalanche of size 6 on any cluster but the largest. An interesting

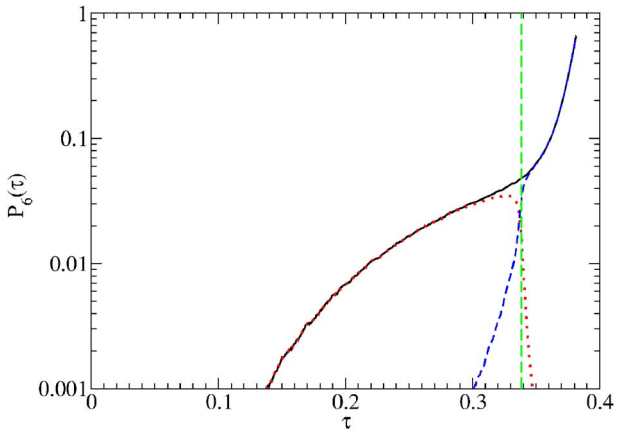

FIG. 7. (Color online) The probability of an avalanche of size 6 (solid line), the probability avalanche of size 6 comes from the largest cluster (dotted line), and their difference (dashed line) for $m=3$ on a triangular lattice. The critical point occurs at the crossover of the latter two curves.

feature of Fig. 7 is the intersection of the latter two curves. At this point there is equal likelihood of having an avalanche of size 6 from the largest cluster as from all other clusters. After this crossover the majority of avalanches of size 6 come from smaller clusters. This crossover occurs very near the BP percolation threshold. Unfortunately, this analysis requires one to label percolation clusters in order to identify the largest one. After τ_c $(p<p_c)$ the SCC, especially the largest cluster, is fractal. Any avalanche on the largest cluster is likely to be large, so small avalanches will likely occur on smaller clusters. For $m=3$ on a cubic lattice, one sees the same crossover at the critical point when considering the contributions to the probability of having an avalanche of size 7, as the smallest stable cluster has eight sites.

IV. DISCUSSION

We have analyzed the behavior of culling avalanches which occur after the death of a single site, in networks where a site is stable provided it has a minimum coordination of m. The culling avalanche distributions for $m=3$ cases on triangular and cubic lattices are qualitatively different than for $m=4$ cases on these lattices. For $m=3$ the culling avalanches have an exponential size distribution [see Figs. 1(b) and 3(b) and Eq. (5)] and the largest avalanche grows as a logarithm of the sample size (see Fig. 5). In contrast the $m=4$ cases have a power law size distribution [see Figs. 2(b) and 4(b) and Eq. (6)] and the largest avalanche grows as the volume of the network (see Fig. 5). The exponent describing the cummulative avalanche distribution at completion is close to 5/2 for the $m=4$ cases on both the triangular and cubic lattices.

We demonstrated that there is an exact relation between the avalanches in bootstrap percolation and the conventional bootstrap percolation point [see Eq. (2)], which requires that we keep account of the number of redundant burnt sites $R(t)$. In first order bootstrap problems, the onset of percolation is marked by the occurrence of an extensive culling avalanche, while in second order cases this does not occur. In the second order cases, we have used a half-interval search to locate p_c, as we did not find any clear change in the behavior of the culling avalanches or avalanche size at p_c.

ACKNOWLEDGMENT

This work has been supported by the DOE under Contract Nos. DE-FG02-90ER45418 and DE-FG02–97ER45651.

[1] J. Chalupa, P. L. Leath, and G. R. Reich, J. Phys. C **12**, L31 (1979).
[2] P. M. Kogut and P. L. Leath, J. Phys. C **14**, 3187 (1981).
[3] B. Pittel, J. Spencer, and N. Wormald, J. Comb. Theory, Ser. B **67**, 111 (1996).
[4] S. Kirkpatrick, W. W. Wilcke, R. B. Garner, and H. Huels, Physica A **314**, 220 (2002).
[5] S. Sabhapandit, D. Dhar, and P. Shukla, Phys. Rev. Lett. **88**, 197202 (2002).
[6] S. S. Manna, Physica A **261**, 351 (1998).
[7] M. Aizenman and J. L. Lebowitz, J. Phys. A **21**, 3801 (1988).
[8] R. H. Shonmann, Ann. Prob. **20**, 174 (1992).
[9] R. Cerf and F. Manzo, Stochastic Proc. Appl. **100**, 69 (2002).
[10] A. E. Holroyd, Probab. Theory Relat. Fields **125**, 195 (2003).
[11] D. Kurtsiefer, Int. J. Mod. Phys. C **14**, 529 (2003).
[12] P. De Gregorio, A. Lawlor, P. Bradley, and K. A. Dawson, Phys. Rev. Lett. **93**, 025501 (2004).
[13] C. M. Chaves and B. Koiller, Physica A **218**, 271 (1995).
[14] M. C. Medeiros and C. M. Chaves, Physica A **234**, 604 (1997).
[15] D. Stauffer and L. de Arcangelis, Int. J. Mod. Phys. C **7**, 739 (1996).
[16] N. S. Branco and C. J. Silva, Int. J. Mod. Phys. C **10**, 921 (1999).
[17] J. Adler and U. Lev, Braz. J. Phys. **33**, 641 (2003).
[18] D. Stauffer and A. Aharony, *Introduction to Percolation Theory*, 2nd ed. (Taylor & Francis, London, 1994).
[19] J. Adler, Physica A **171**, 453 (1991).
[20] J. Adler, D. Stauffer, and A. Aharony, J. Phys. A **22**, L297 (1989).
[21] S. S. Manna, D. Stauffer, and D. W. Heermann, Physica A **162**, 20 (1989).
[22] J. Hoshen and R. Kopelman, Phys. Rev. B **14**, 3438 (1976).